# Engineering SYK Interactions in Disordered Graphene Flakes under Realistic Experimental Conditions

Marta Brzezińska,[1] Yifei Guan,[1] Oleg V. Yazyev,[1] Subir Sachdev,[2] and Alexander Kruchkov[1,2,3]
[1]Institute of Physics, Ecole Polytechnique Fédérale de Lausanne (EPFL), CH-1015 Lausanne, Switzerland
[2]Department of Physics, Harvard University, Cambridge, Massachusetts 02138, USA
[3]Branco Weiss Society in Science, ETH Zurich, Zurich, CH 8092, Switzerland

(Received 5 January 2023; accepted 19 May 2023; published 18 July 2023)

We model interactions following the Sachdev-Ye-Kitaev (SYK) framework in disordered graphene flakes up to 300 000 atoms in size (∼100 nm in diameter) subjected to an out-of-plane magnetic field $B$ of 5–20 Tesla within the tight-binding formalism. We investigate two sources of disorder: (i) irregularities at the system boundaries, and (ii) bulk vacancies—for a combination of which we find conditions that could be favorable for the formation of the phase with Sachdev-Ye-Kitaev features under realistic experimental conditions above the liquid helium temperature.

DOI: 10.1103/PhysRevLett.131.036503

There has been significant recent interest in the condensed matter community of a holographic gravitational description of correlated electron systems [1,2]. A model in this direction is the Sachdev-Ye-Kitaev (SYK) model [3,4], which describes from the condensed matter perspective a set of $N$ electrons in a dispersionless quantum state (a flat band), interacting strongly yet randomly all to all,

$$\mathcal{H}_{\mathrm{SYK}} = \sum_{ijkl}^{N} J_{ijkl} c_i^\dagger c_j^\dagger c_k c_l. \tag{1}$$

Here, $c_i^\dagger$ ($c_i$) are fermionic creation (annihilation) operators, and $J_{ijkl}$ are random couplings in all indices (the model works beyond the Gaussian randomness [5]). Despite its attractive mathematical properties such as exact solvability in the large $N$ limit with nearly conformal properties [6,7], mapping on the Jackiw-Teitelboim gravity [8], and importance for condensed matter physics (including strange metallicity [9–11] and superconductivity on the basis of SYK model [12–14]), a direct experimental realization is currently missing.

Various theoretical simulations for the physical realization of the SYK model have been discussed [15–20]. Among them, a promising potential experimental platform for the electronic SYK model, given in Ref. [20], is a graphene dot with irregular boundaries placed in an external magnetic field. Reference [20] studied ∼2000 atoms (5 nm in radius) in a field of ∼3200 T. However, the magnetic fields employed in Ref. [20] exceed capabilities within the laboratory realm. Modern condensed matter facilities operate with quantum transport at magnetic fields up to 16–20 T, and the highest accessible magnetic fields in dc operation are of 45 T [21]. At the same time, graphene preparation and chemical etching procedures pose limits on the controllable size and shape of a flake, allowing flexible operational capabilities with flake sizes of 100 nm and above, but not for a size of a few nanometers. In this regard, a great challenge is to overcome these obstacles to engineer a realistic graphene flake that could host relevant interactions in the experimentally accessible magnetic fields of 5–20 T.

In this Letter we report large-scale calculations on large graphene flakes involving up to 300 000 carbon atoms (corresponding to flake size ≈100 nm) placed under realistic experimental conditions. We find that upon choosing a well-disordered flake, we can reach favorable experimental conditions with SYK strength $J \sim 45$ meV (we use standard normalization $J^2 = 2N^3\langle|J_{ijkl}|^2\rangle$), and a mesoscopic number of SYK fermions $N$, typically around 40 in our calculations in the magnetic fields of 10–20 T. We further model (i) the role of chemical etching [22], or local anodic oxidation with an atomic force microscopy tip [23–25], by varying the shape of the flake and the size of edge disorder and (ii) the role of bulk vacancies created, for example, by focused ion beam (FIB) patterning [26] or hydrogen plasma treatment [27]. Our results speak in favor of formation of SYK-like interactions in the realistic range of parameters. In particular, we point out how the relative effect of melonic diagrams can be enforced by controlling the atomic vacancies concentration in the bulk. By comparing the relevant energy scales [28], namely $t^2/J$ and $J/N$, we come to the conclusion that the engineered system has a set of parameters where it could realize the SYK phase in the vicinity of the liquid helium operational temperatures, accessible magnetic fields, and suitable graphene flake scales.

*Setup.*—To construct the SYK model, one needs to employ the dispersionless quantum states (flat bands). The electronic states with nontrivial Bloch topology are

 © 2023 American Physical Society

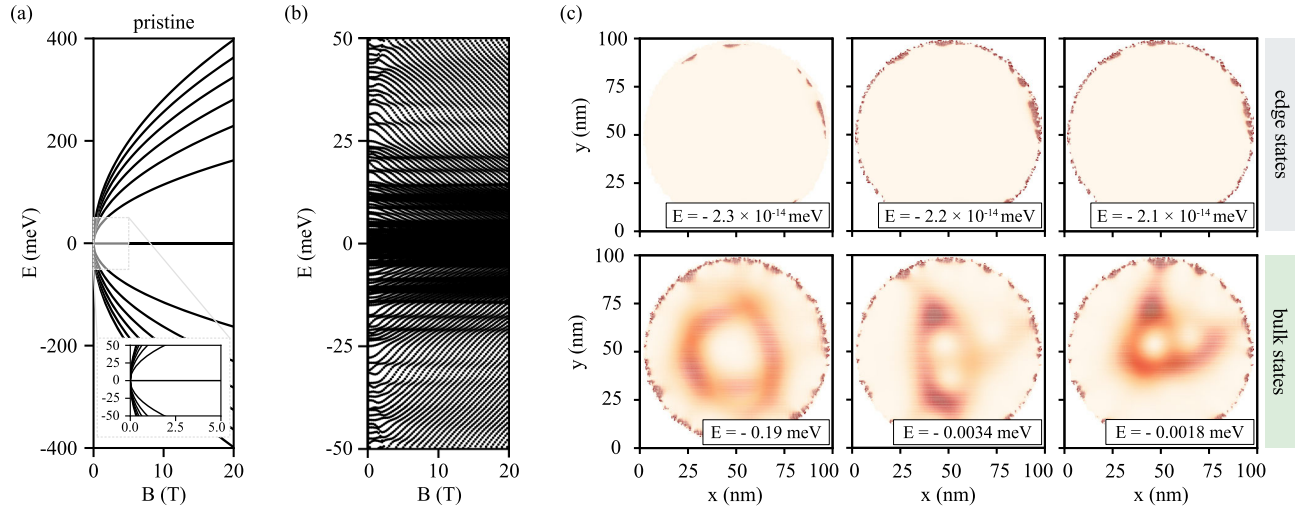


FIG. 1. Bulk and edge states in disordered graphene flake of 100 nm in strong magnetic fields. (a) Energy spectrum as a function of magnetic field, expected in pristine graphene; inset shows the same spectrum in energy range −50 to +50 meV to compare with panel (b). (b) De facto energy spectrum, observed in a strongly disordered graphene flake of size 100 nm; higher Landau levels ($|n| > 0$) are not recognized in the energy range −50 to +50 meV. (c) Probability densities $|\psi|^2$ of exemplary bulk and edge states. Randomly localized bulk states shown in bottom of (c) are the building blocks for constructing the SYK-like interactions (Fig. 2).

preferred for our purpose as they are spread over multiple atomic sites and are immune to Anderson localization [29]. Such flat band states have been classified in Ref. [30]. The simplest of this construction are the Landau levels, which are characterized by Chern number $|C| = 1$. In principle, one can use numerous 2D materials for this purpose. However we here limit ourself to the case of graphene [20] for two reasons: (i) graphene monolayer is an intuitively understood system from both analytical and numerical viewpoints, and (ii) there are existing experimental platforms satisfying criteria for this direction [31,32].

Before proceeding to disordered graphene flakes, let us recall the physics of pristine (homogeneous and boundless) graphene in low-energy approximation. Upon application of out-of-plane magnetic field $B$, the electronic spectrum of pristine graphene is given by [33]

$$E_n = \pm v_F \sqrt{2\hbar e B|n|}, \tag{2}$$

where $e$ is electronic charge and $v_F \approx 10^6$ m/s is the Fermi velocity. The lowest Landau level (LLL) is characterized by zero modes in the bulk ($n = 0$). In the presence of chiral symmetry, the Aharonov-Casher argument [34] sets the number of electronic states in LLL as

$$N_0 = \frac{BA}{\Phi_0}, \tag{3}$$

where $A$ is the flake area, and $\Phi_0 = h/e = 4.136 \times 10^{-15}$ Wb is the magnetic flux quantum. $N_0$ in Eq. (3) sets the order of magnitude for the number $N$ of SYK states in the Hamiltonian in Eq. (1). However, we see that $N$ within bandwidth $t = 2$ meV around the Fermi level $N$ is fluctuating around $N_0$ due to strong disorder effects in considered graphene flakes (see Fig. 2). Still there is a certain qualitative similarity with the ideal LLL case, even that the flake is strongly disordered.

The typical electronic spectrum of a strongly disordered graphene flake is illustrated in Fig. 1. The flake has a disorder-free inner region of radius $R_1$, followed by disordered edge up to radius $R_2$ (46 nm and 50 nm in Figs. 1 and 2). Tight-binding calculations are performed with the conventional graphene model in magnetic fields [35], taking into account nearest-neighbor hoppings with Peierls substitution. Disorder is modeled by the random on-site term $\sum_i V_i c_i^\dagger c_i$ with $V_i \to \infty$, where the $V_i$ is either applied to the $i$th site in the bulk region (defined by the radius $R_1$) or at the edge (within $R_2 - R_1$) [36]. Figure 1 shows the results obtained from diagonalization of the tight-binding model describing the 100 nm flake consisting of around 270 000 atoms. The first observation is that the electronic spectrum of a realistic disordered flake in the relevant energy range deviates significantly from its pristine counterpart, given by Eq. (2): in all the realistic magnetic fields 0–20 T, we no longer observe the square-root behavior of eigenenergies as expected for pristine graphene; instead, the spectrum acquires a quantum-dot-like distribution [39].

We distinguish the bulk states from the edge states through the analysis of their localization properties. For this, we integrate $|\Psi|^2$ within radius $R_1 + \delta$ ($\delta \to 0$) [49]. Because of the presence of irregularities on the boundaries, all the states are showing certain localization at the edge. However, bulk states have significant weight in bulk. If at least 50% of weight is localized in bulk, we label this state as a bulk state. While, as expected, the edge states are strongly localized at the irregular boundaries, the bulk

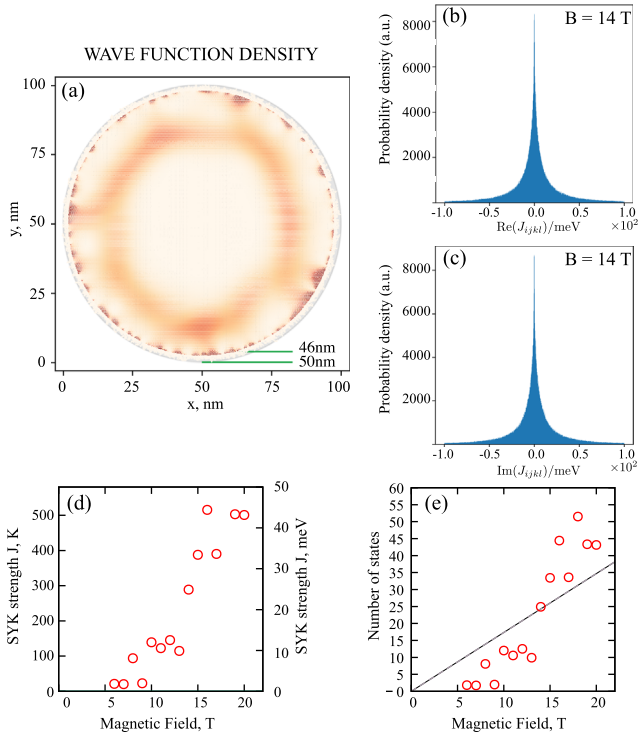


FIG. 2. SYK-like interactions in the graphene flake of size 100 nm (268 510 carbon atoms) under realistic magnetic fields 5–20 T. (a) The geometry of the flake used for numerical modeling, together with the visualization of a typical bulk state near the Fermi level. (b),(c) Distribution of real and imaginary parts $J_{ijkl}$ terms computed from Eq. (4) with $\mathrm{Re}\langle J_{ijkl}\rangle \approx 0$ and $\mathrm{Im}\langle J_{ijkl}\rangle \approx 0$. (d) The value of SYK interaction $J$, determined by the second moments in Eq. (5). For calculation, we take bulk states distributed between $-1$ and $+1$ meV around the Fermi level. Panel (e) shows number of bulk states in the range $-1$ to $+1$ meV involved into $J_{ijkl}$ calculation; gray dashed line depicts ideal LLL case [Eq. (3)].

states sway over all the flake diameter, being spread on the length scale of ~100 nm. With such large length scale over which the bulk states are spread, the notion of distance is lost, and these states are interacting randomly all to all in the SYK spirit.

*Calculation of the SYK terms.*—With the bulk states randomly localized, and the kinetic energy quenched to $t < 2$ meV, we construct the SYK-like states by introducing the Coulomb interaction in the basis of randomized bulk states [20,50]. We compute Sachdev-Ye-Kitaev interaction terms through [40]

$$J_{ijkl} = \frac{1}{2}\sum_{\boldsymbol{r}_1}\sum_{\boldsymbol{r}_2}\Psi_i^*(\boldsymbol{r}_1)\Psi_j^*(\boldsymbol{r}_2)U(\boldsymbol{r}_1-\boldsymbol{r}_2)\Psi_k(\boldsymbol{r}_1)\Psi_l(\boldsymbol{r}_2), \quad (4)$$

where $U(\boldsymbol{r})$ is the screened Coulomb potential. Our results stand for different forms of the screened Coulomb potentials. To be specific, we adopt the values of renormalized interaction potentials for graphene as it was reported in Ref. [51]. In particular, we adopt $U_{\mathrm{NN}} = 5.5$ eV, $U_{\mathrm{NNN}} = 4.1$ eV, and $U_{\mathrm{NNNN}} = 3.6$ eV, where NN, NNN, and NNNN stand for nearest-neighbor, next-to-nearest neighbor, and next-to-next-to-nearest-neighbor interactions, respectively. In calculation of $J_{ijkl}$ terms [Eq. (4)], we take only bulk states within the energy range $-1$ to $+1$ meV around the neutrality. This qualitatively corresponds to focusing on the states associated with what used to be LLL [see dashed line in Fig. 2(e)], similar to Ref. [20]. For medium size flakes, we check that changing the bulk states range from between $-1$ and $+1$ meV to between $-5$ and $+5$ meV does not change significantly the results for $J_{ijkl}$ calculations, since most of the bulk states are situated near the zero energy, and higher excited bulk states contribute marginally to SYK interactions $J_{ijkl}$. Hence, in what follows we proceed with bulk states within the $-1$ to $+1$ meV range.

The key results for the large flake are summarized in Fig. 2. The statistical distribution of the complex-valued $J_{ijkl}$ terms is illustrated in Figs. 2(b) and 2(c). The mean is zero, ($\mathrm{Re}\ \langle J_{ijkl}\rangle \approx 0$, $\mathrm{Im}\ \langle J_{ijkl}\rangle \approx 0$), which indicates that real and imaginary parts of $J_{ijkl}$ are independent. The overall distribution of the absolute values of $J_{ijkl}$ is quasirandom but non-Gaussian as in conventional SYK models [6,7]. However, this is not the problem for constructing SYK-like models [5]. We introduce the real-valued strength of SYK interactions $J$ as with normalization from counting melonic diagrams [7]:

$$J = \sqrt{2}N^{3/2}\langle J_{ijkl}J_{ijkl}^*\rangle^{1/2}. \quad (5)$$

We operate this quantity in meV and Kelvin for practical convenience. The results for the large flake are encouraging, with extracted $J$ of around 35 meV at 15 T [see Fig. 2(d)]. The number of SYK fermions peaks to between 50 and 60 and we typically take around 40 of them for our calculations.

*Dependence on edge disorder scale.*—We next address the question of how the edge disorder $\chi = (R_2 - R_1)/R_2$ influences the SYK interaction strength $J$. This question is vital for the experiments, where only a limited number of methods is available for shaping the flake of the size of 100–200 nm (chemical etching, FIB, hydrogen plasma treatment). To optimize the numerical costs, we now turn to the medium size flakes of diameter 80 nm (~150 000 atoms); these results are rescalable towards large graphene flake of size 300 000 atoms and more as in prototypes [31]. We observe that the strength of the SYK interaction $J$ can be tuned by increasing the edge disorder $\chi$ (see Fig. 3). To quantify this effect we perform disorder averaging over dozens of flakes (Fig. 3 uses up to 30-40 flake realizations) [52]. Typically $J$ scatters from 20 meV to nearly 60 meV upon increasing $\chi$ from 0 to 20%, but some samples may exhibit even larger values of $J$ above a hundred meV (outside of plot range in Fig. 3) at moderate

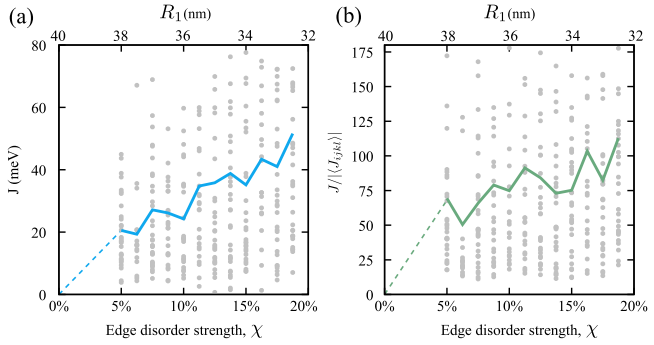


FIG. 3. Enhancing SYK interactions through edge disorder $\chi$. (a) SYK coupling strength $J$; (b) dimensionless ratio $J/|\langle J_{ijkl}\rangle|$ as a function of edge disorder scale $\chi$ for the medium size flake at $B = 20$ T (approximately 150 000 atoms, 80 nm in diameter). Solid lines correspond to the average over up to 20 disorder realizations (marked with gray points, some outside of plot range). In this figure, the flake has dimensions $R_2 = 40$ nm (outer radius), and $R_1$ changes from 33 to 38.5 nm (inner radius).

edge disorders. For 40 nm flakes presented in Fig. 3, we cannot access data for $R_1 \approx 39$ nm, as it is hard to separate contributions from the edge states and the bulk states; the edge states have finite penetration depth into the bulk of the flake, see Fig. 1. Physically, the value of $J$ should drop to zero for a pristine flake ($R_1 = R_2$), this is depicted with a dashed line which serves as a guide for eyes. Comparing Figs. 3 with 2, we come to the conclusion that the energy scale $J \sim 20$–$40$ meV is the most robust for the experiments, as it persists in the broad range of edge disorder (the value and uncertainties of which is hard to control experimentally). Moreover, the ratio of $J/|\langle J_{ijkl}\rangle|$ in Fig. 3(b), which qualitatively points to the dominance of the melonic diagrams in the large-$N$ limit, increases under edge disorder.

*Enhancing the role of melonic diagrams.*—Implanting bulk vacancies in the flake offers a powerful means to control the strength of effective SYK interactions (4). In practice, this technique could be implemented using the FIB tool. In this case, the sample patterning can provide additional tuning knob to improve the properties toward SYK-like behavior. We here perform the calculations for the medium size flakes of 80 nm in $B = 20$ T. The results are shown in Fig. 4. We start with the flake that has only moderate (nonoptimized) edge disorder, reflected in $J \approx 20$ meV, and gradually increase the number of atomic vacancies (indicated in percent). Figure 4(b) gives the dependence of the SYK interaction $J$ versus vacancy concentration in the bulk. The SYK coupling strength $J$ is around 20 meV throughout the disorder range. The number of bulk states slowly grows with a vacancy concentration; we check that the bulk states are not exponentially localized on the atomic vacancies. Figure 4(c) presents the ratio of couplings $J/|J_{ijkl}|$. While the coupling strength $J$ fluctuates moderately around its original value, the ratio $J/|\langle J_{ijkl}\rangle|$ is significantly improved by adding a moderate amount of vacancies (at 0% this ratio is $J/|\langle J_{ijkl}\rangle| \approx 50$, at 5% it is $J/|\langle J_{ijkl}\rangle| \approx 200$), hence promoting the role of melonic diagrams [7]. Therefore, we come to the conclusion that even a modest vacancy concentration of 5% can improve the properties of the SYK flake. For the flakes of size 100 nm (∼300 000 atoms), we recommend removing ∼15 000 to ∼30 000 carbon atoms.

*Discussion of the temperature scales.*—Finally, we perform the analysis of the relevant energy scales. The key energy scale is $J \approx 35$ meV (taken at experimentally relevant $B = 16$ T from Fig. 2). The SYK model is well-defined in the region $T \ll J$. Furthermore, there are lower bounds on the temperature coming from (i) finite bandwidth of the flat band, and (ii) mesoscopic effects in the SYK Hamiltonians. Both these temperature scales appear in quantum transport treatment of the SYK island [28]. The first temperature bound is set by the bandwidth $t$. However,

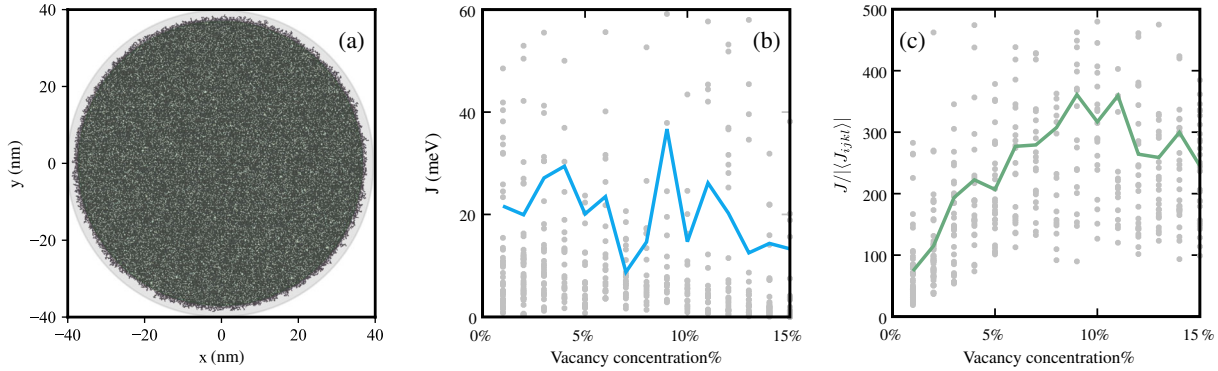


FIG. 4. Tuning SYK strength $J$ with vacancy patterning. (a) Illustration of the graphene flake with 10% bulk atomic vacancies (diameter 80 nm, approximately 156 000 atoms), (b) SYK strength $J$, and (c) $J/|\langle J_{ijkl}\rangle|$ ratio as a function of the vacancies concentration in the range from 0% to 15% of vacancies. Solid blue lines correspond to arithmetic average over 20 disorder realizations in the medium size flake with $R_1 = 37$ nm and $R_2 = 40$ nm at $B = 20$ T [some sample points (gray) are outside of the plot range]. Above 15%, the long-range order is destroyed for some disorder realizations and around 30%. All the systems are close to the percolation threshold for hexagonal lattice $p \approx 0.7$ [53,54].

the question of the bandwidth for strongly disordered flakes is not well-defined. From Fig. 1(b) we estimate the upper bound as $\pm 15$ meV, from which we estimate $t \approx 7.5$ meV; similar upper bounds are imposed by experiment [55]. This gives $T_1 = t^2/J \approx 19$ K. Around this value, the SYK dynamics cross over to conventional Fermi liquid behavior in a universal manner. The second temperature scale is set by the mesoscopic number of SYK states. In our case of a large flake ($N \approx 35$), $T_2 = J/N \approx 10$ K. Below $T_2$, mesoscopic fluctuations are described by the universal Schwarzian theory of the SYK model (with possible perturbations from $t$) [28]. Therefore, we come to the conclusion that in the magnetic fields of 16 T, flake sizes of order 100 nm, the SYK dynamics is most favorable in the regime $20\ \mathrm{K} \lesssim T_{\mathrm{SYK}} \ll 300$ K. We hence expect the signatures of SYK model [7] in this temperature range, and probe the relevant quantum transport, namely anomalies in thermopower, in this setup [28]; see [56–60] for a similar setup. This allows one to operate the 100 nm graphene flakes of Figs. 1 and 2 above the point of the liquid helium temperature ($T_{\mathrm{He}} = 4.2$ K), a relevant experimental benchmark.

*Conclusions.*—In conclusion, by performing large-scale calculations on up to 300 000 atomic sites, we have demonstrated that the SYK interactions can be controllably engineered and enhanced in the disordered graphene flake in realistic magnetic fields 5–20 T when the flake enters the quantum dot regime. The obtained results speak in favor of underlying SYK dynamics in the disordered graphene flakes, establishing realistic experimental conditions in terms of length scales, temperatures, and magnetic fields. Further theoretical modeling of transport across such disordered graphene flakes is required to interpret the graphene prototype behavior in experiments [31].

We thank Philip Kim, Bertrand Halperin, Laurel Anderson for useful discussion. This work was supported by the Branco Weiss Society in Science, ETH Zurich, through the research grant on flat bands, strong interactions, and the SYK physics. Computations have been performed at the Swiss National Supercomputing Centre (CSCS), project S1146, and the facilities of Scientific IT and Application Support Center of EPFL. S. S. was supported by the National Science Foundation under Grant No. DMR-2002850 and by the Simons Collaboration on Ultra-Quantum Matter, a grant from the Simons Foundation (651440). Y. G. and O. V. Y. acknowledge support from the Swiss National Science Foundation (Grant No. 204254).

M. B. and Y. G. contributed equally to this work.

[1] S. A. Hartnoll, A. Lucas, and S. Sachdev, *Holographic Quantum Matter* (MIT Press, Cambridge, MA, 2018).
[2] S. A. Hartnoll, Classical Quantum Gravity **26**, 224002 (2009).
[3] S. Sachdev and J. Ye, Phys. Rev. Lett. **70**, 3339 (1993).
[4] A. Y. Kitaev, *Entanglement in strongly-correlated quantum matter, Talks at KITP* (University of California, Santa Barbara, 2015).
[5] T. Krajewski, M. Laudonio, R. Pascalie, and A. Tanasa, Phys. Rev. D **99**, 126014 (2019).
[6] J. Maldacena and D. Stanford, Phys. Rev. D **94**, 106002 (2016).
[7] Y. Gu, A. Kitaev, S. Sachdev, and G. Tarnopolsky, J. High Energy Phys. 02 (2020) 157.
[8] A. Kitaev and S. J. Suh, J. High Energy Phys. 05 (2018) 183.
[9] A. Haldar and V. B. Shenoy, Phys. Rev. B **98**, 165135 (2018).
[10] P. Cha, N. Wentzell, O. Parcollet, A. Georges, and E.-A. Kim, Proc. Natl. Acad. Sci. U.S.A. **117**, 18341 (2020).
[11] D. Chowdhury, A. Georges, O. Parcollet, and S. Sachdev, Rev. Mod. Phys. **94**, 035004 (2022).
[12] H. Wang, A. L. Chudnovskiy, A. Gorsky, and A. Kamenev, Phys. Rev. Res. **2**, 033025 (2020).
[13] L. Classen and A. Chubukov, Phys. Rev. B **104**, 125120 (2021).
[14] G.-A. Inkof, K. Schalm, and J. Schmalian, NPG Quantum Mater. **7**, 56 (2022).
[15] A. Chew, A. Essin, and J. Alicea, Phys. Rev. B **96**, 121119 (2017).
[16] D. I. Pikulin and M. Franz, Phys. Rev. X **7**, 031006 (2017).
[17] I. Danshita, M. Hanada, and M. Tezuka, Prog. Theor. Exp. Phys. **2017**, 083I01 (2017).
[18] L. García-Álvarez, I. L. Egusquiza, L. Lamata, A. del Campo, J. Sonner, and E. Solano, Phys. Rev. Lett. **119**, 040501 (2017).
[19] Z. Luo, Y.-Z. You, J. Li, C.-M. Jian, D. Lu, C. Xu, B. Zeng, and R. Laflamme, npj Quantum Inf. **5**, 53 (2019).
[20] A. Chen, R. Ilan, F. de Juan, D. Pikulin, and M. Franz, Phys. Rev. Lett. **121**, 036403 (2018).
[21] S. Hahn, K. Kim, K. Kim, X. Hu, T. Painter, I. Dixon, S. Kim, K. R. Bhattarai, S. Noguchi, J. Jaroszynski *et al.*, Nature (London) **570**, 496 (2019).
[22] L. Wang, I. Meric, P. Huang, Q. Gao, Y. Gao, H. Tran, T. Taniguchi, K. Watanabe, L. Campos, D. Muller *et al.*, Science **342**, 614 (2013).
[23] R. Puddy, P. Scard, D. Tyndall, M. Connolly, C. Smith, G. Jones, A. Lombardo, A. Ferrari, and M. Buitelaar, Appl. Phys. Lett. **98**, 133120 (2011).
[24] S. Masubuchi, M. Arai, and T. Machida, Nano Lett. **11**, 4542 (2011).
[25] H. Li, Z. Ying, B. Lyu, A. Deng, L. Wang, T. Taniguchi, K. Watanabe, and Z. Shi, Nano Lett. **18**, 8011 (2018).
[26] B. Archanjo, A. Barboza, B. Neves, L. Malard, E. Ferreira, J. Brant, E. Alves, F. Plentz, V. Carozo, B. Fragneaud *et al.*, Nanotechnology **23**, 255305 (2012).
[27] E. Despiau-Pujo, A. Davydova, G. Cunge, and D. B. Graves, Plasma Chem. Plasma Process. **36**, 213 (2016).
[28] A. Kruchkov, A. A. Patel, P. Kim, and S. Sachdev, Phys. Rev. B **101**, 205148 (2020).
[29] The topological flat band condition is an unnecessary but desired condition for the SYK construction. A good combination of Coulomb interaction and moderate disorder

in such bands enhances the effective values of SYK interactions, $J$, compared to topologically trivial bands.
[30] A. Kruchkov, Phys. Rev. B **105**, L241102 (2022).
[31] L. Anderson, A. Laitinen, A. Kruchkov, K. Watanabe, T. Taniguchi, and P. Kim, Bull. Am. Phys. Soc. **67** (2022), https://meetings.aps.org/Meeting/MAR22/Session/D56.6.
[32] L. E. Anderson, Electrical and thermoelectric transport in mixed-dimensional graphitic mesoscopic systems, Ph.D. thesis, Harvard University, 2022.
[33] V. P. Gusynin and S. G. Sharapov, Phys. Rev. Lett. **95**, 146801 (2005).
[34] Y. Aharonov and A. Casher, Phys. Rev. A **19**, 2461 (1979).
[35] M. O. Goerbig, Rev. Mod. Phys. **83**, 1193 (2011).
[36] For computational advance, we combine KWANT toolbox [37] with FEAST algorithms [38].
[37] C. W. Groth, M. Wimmer, A. R. Akhmerov, and X. Waintal, New J. Phys. **16**, 063065 (2014).
[38] E. Polizzi, Phys. Rev. B **79**, 115112 (2009).
[39] We note, however, that in much stronger magnetic flux $\sim h/e$, the well-defined structure from Eq. (2) reappears [40].
[40] See Supplemental Material at http://link.aps.org/supplemental/10.1103/PhysRevLett.131.036503 for details on numerical calculations, which includes Refs. [41–48].
[41] A. H. Castro Neto, F. Guinea, N. M. R. Peres, K. S. Novoselov, and A. K. Geim, Rev. Mod. Phys. **81**, 109 (2009).
[42] A. F. Young, C. R. Dean, L. Wang, H. Ren, P. Cadden-Zimansky, K. Watanabe, T. Taniguchi, J. Hone, K. L. Shepard, and P. Kim, Nat. Phys. **8**, 550 (2012).
[43] G. Tarnopolsky, A. J. Kruchkov, and A. Vishwanath, Phys. Rev. Lett. **122**, 106405 (2019).
[44] S. Schnez, K. Ensslin, M. Sigrist, and T. Ihn, Phys. Rev. B **78**, 195427 (2008).
[45] M. van Schilfgaarde and M. I. Katsnelson, Phys. Rev. B **83**, 081409(R) (2011).
[46] B. Gavin and E. Polizzi, Numer. Linear Algebra Appl. **25**, e2188 (2018).
[47] E. Polizzi, Phys. Rev. B **79**, 115112 (2009).
[48] S. Sahoo, E. Lantagne-Hurtubise, S. Plugge, and M. Franz, Phys. Rev. Res. **2**, 043049 (2020).
[49] For numerical purposes, we use $\delta = 0.1(R_2 - R_1)$ in the calculations in the main text.
[50] C. Wei and T. A. Sedrakyan, Phys. Rev. A **103**, 013323 (2021).
[51] T. O. Wehling, E. Şaşıoğlu, C. Friedrich, A. I. Lichtenstein, M. I. Katsnelson, and S. Blügel, Phys. Rev. Lett. **106**, 236805 (2011).
[52] At tiny edge disorder level, the bulk modes are mixed with the contribution from edge states. Thus, the $J$ terms become very large.
[53] P. N. Suding and R. M. Ziff, Phys. Rev. E **60**, 275 (1999).
[54] X. Feng, Y. Deng, and H. W. J. Blöte, Phys. Rev. E **78**, 031136 (2008).
[55] Y. Zhang, Z. Jiang, J. P. Small, M. S. Purewal, Y.-W. Tan, M. Fazlollahi, J. D. Chudow, J. A. Jaszczak, H. L. Stormer, and P. Kim, Phys. Rev. Lett. **96**, 136806 (2006).
[56] N. V. Gnezdilov, J. A. Hutasoit, and C. W. J. Beenakker, Phys. Rev. B **98**, 081413 (2018).
[57] A. Altland, D. Bagrets, and A. Kamenev, Phys. Rev. Lett. **123**, 226801 (2019).
[58] O. Can, E. M. Nica, and M. Franz, Phys. Rev. B **99**, 045419 (2019).
[59] A. I. Pavlov and M. N. Kiselev, Phys. Rev. B **103**, L201107 (2021).
[60] C. Zanoci and B. Swingle, Phys. Rev. B **105**, 235131 (2022).